Luminescent Gold(I) Acetylides: From Model Compounds to Polymers

Michael J. Irwin, Jagadese J. Vittal, and Richard J. Puddephatt*

Department of Chemistry, University of Western Ontario, London, Canada N6A 5B7

Received March 25, 1997[⊗]

The emission spectra of rigid-rod, conjugated polymeric complexes of gold(I) of the type $[-Au-C{\equiv}C-Ar-C{\equiv}C-Au-L-L-]_x$, where Ar = aryl and L−L = diphosphine or bis(isocyanide) ligands are reported for the first time, along with the corresponding spectra of analogous mononuclear and binuclear alkynylgold(I) model complexes. It is found that the emission spectra display a red shift on going from mononuclear to binuclear to polynuclear structures, and it is tentatively argued that this provides evidence for extended π-conjugation in the polymers. Many of the model complexes display a red shift in the emission spectra on going from solution in dichloromethane to the solid state; in most cases, this is attributed to the presence of intermolecular Au···Au bonding in the solid state but, in one case, it is also observed when the intermolecular Au···Au distance is too long to be consistent with a bonding interaction. Assignments of the emission spectra are aided by EHMO (extended Hückel molecular orbital) calculations on model complexes. Structures of the model complexes $[Me_3P-Au-C{\equiv}C-C_6H_2Me_2-C{\equiv}C-Au-PMe_3]$, the first digold diacetylide to be structurally characterized, and $[XyN{\equiv}C-Au-C{\equiv}C-C_6H_4-NO_2]$ have been determined crystallographically.

Introduction

There has been great interest in organogold chemistry recently, and the most active topics include studies of weak gold···gold bonding interactions in gold(I) complexes and how these can affect conformations, crystal packing and chemical reactions,[1−7] and studies of the luminescence of gold(I) compounds.[8−13] In some cases, a relationship between the two effects has been suggested, namely that luminescence is likely to be observed when the gold···gold interactions are present.[8,11] This is most easily understood if the emission is from a metal-based excited state, but emission has also been proposed to occur from $\sigma-\pi^*$, $\pi-\pi^*$, or LMCT (ligand to metal charge transfer) excited states in different complexes.[8−13] Emission has been observed from complexes containing from 1−4 gold(I) centers but not yet from polymeric gold complexes.[8−13] The synthesis of rigid-rod polymers with gold(I) centers bridged by diacetylides with either diisocyanides[14] or diphosphines[15] has been reported recently, along with some model compounds containing the same structural units L−Au−C≡C−Ar−C≡C−Au−L, L = isocyanide or phosphine ligand, or R−C≡C−Au−L−L−Au−C≡C−R, L−L = diisocyanide or diphosphine.[14−16] The polymers are easily prepared but are insoluble in common organic solvents. Hence, their characterization is based partly on comparison of spectroscopic properties with those of the model compounds, and since the model compounds usually contain intermolecular Au···Au interactions, it is proposed that the polymers do also.[14,15]

Since several recent reports have established that alkynylgold(I) complexes containing phosphine or isocyanide ligands exhibit strong emission spectra,[8,9] it was of interest to investigate the photophysics of the above model compounds and rigid-rod polymers for comparison. This paper reports the results of this first study of the emission spectra of rigid-rod gold polymers and also the structures of two more model compounds,

[⊗] Abstract published in *Advance ACS Abstracts,* July 1, 1997.

(1) (a) Li, J.; Pyykko, P. *Chem. Phys. Lett.* **1992**, *197*, 586. (b) Pathaneni, S. S.; Desiraju, G. R. *J. Chem. Soc., Dalton Trans.* **1993**, 319.

(2) (a) Schmidbaur, H.; Graf, W.; Muller, G. *Angew. Chem., Int. Ed. Engl.* **1988**, *27*, 417. (b) Schmidbaur, H.; Dziwok, K.; Grohmann, A.; Muller, G. *Chem. Ber.* **1989**, *122*, 893. c) Sladek, A.; Schmidbaur, H. *Inorg. Chem.* **1996**, *35*, 3268.

(3) Veiros, L. F.; Calhorda, M. J. *J. Organomet. Chem.* **1996**, *510*, 71.

(4) Payne, N. C.; Ramachandran, R.; Puddephatt, R. J. *Can. J. Chem.* **1995**, *73*, 6.

(5) Mingos, D. M. P.; Yau, J.; Menzer, S.; Williams, D. J. *Angew. Chem., Int. Ed. Engl.* **1995**, *34*, 1894.

(6) Van Calcar, P. M.; Olmstead, M. M.; Balch, A. L. *J. Chem. Soc., Chem. Commun.* **1995**, 1773.

(7) Irwin, M. J.; Rendina, L.; Vittal, J. J.; Puddephatt, R. J. *J. Chem. Soc., Chem. Commun.* **1996**, 1281.

(8) (a) Shieh, S. J.; Hong, X.; Peng, S. M.; Che, C. M. *J. Chem. Soc., Dalton Trans.* **1994**, 3067. (b) Che, C. M.; Yip, H. K.; Wong, W. T.; Lai, T. F. *Inorg. Chim. Acta* **1992**, *197*, 177. (c) Xiao, H.; Cheung, K.-K.; Che, C.-M. *J. Chem. Soc., Dalton Trans.* **1996**, 3699. (d) Tzeng, B.-C.; Lo, W.-C.; Che, C.-M.; Peng, S.-M. *J. Chem. Soc., Chem. Commun.* **1996**, 181. (e) Li, D.; Hong, X.; Che, C.-M.; Lo, W.-C.; Peng, S.-M. *J. Chem. Soc., Dalton Trans.* **1993**, 2929. (f) Che, C.-M.; Yip, H.-K.; Lo, W.-C.; Peng, S.-M. *Polyhedron* **1994**, *13*, 887.

(9) (a) Yam, V. W. W.; Choi, S. W. K.; Cheung, K. K. *Organometallics* **1996**, *15*, 1734. (b) Muller, T. E.; Choi, S. W. K.; Mingos, D. M. P.; Murphy, D.; Williams, D. J.; Yam, V. W. W. *J. Organomet. Chem.* **1994**, *484*, 209. (c) Yam, V. W.-W.; Choi, S. W.-K. *J. Chem. Soc., Dalton Trans.* **1996**, 4227.

(10) Perreault, D.; Drouin, M.; Michel, A.; Harvey, P. D. *Inorg. Chem.* **1991**, *30*, 2.

(11) (a) King, C.; Wang, J. C.; Khan, M. N. I.; Fackler, J. P., Jr. *Inorg. Chem.* **1989**, *28*, 2145. (b) Assefa, Z.; Staples, R. J.; Fackler, J. P., Jr. *Inorg. Chem.* **1994**, *33*, 2790.

(12) (a) Hanna, S. D.; Khan, S. I.; Zink, J. I. *Inorg. Chem.* **1996**, *35*, 5813. (b) Feng, D.-F.; Tang, S. S.; Liu, C. W.; Lin, I. J. B.; Wen, Y.-S.; Liu, L.-K. *Organometallics* **1997**, *16*, 901.

(13) Jones, W. B.; Yuan, J.; Narayanaswamy, R.; Young, M. A.; Elder, R. C.; Bruce, A. E.; Bruce, M. R. M. *Inorg. Chem.* **1995**, *34*, 1996.

(14) Irwin, M. J.; Jia, G.; Payne, N. C.; Puddephatt, R. J. *Organometallics* **1996**, *15*, 51.

(15) Jia, G.; Puddephatt, R. J.; Scott, J.; Vittal, J. J. *Organometallics* **1993**, *12*, 3565.

(16) Jia, G.; Payne, N. C.; Puddephatt, R. J.; Vittal, J. J. *Organometallics* **1993**, *12*, 4771.

S0276-7333(97)00256-2 CCC: $14.00

$[Me_3P-Au-C\equiv C-C_6H_2Me_2-C\equiv C-Au-PMe_3]$, the first digold diacetylide to be structurally characterized, and $[XyN\equiv C-Au-C\equiv C-C_6H_4-NO_2]$.

Experimental Section

All complexes were synthesized and characterized by the methods reported previously.[14−16] Emission spectra were recorded at room temperature by using a PTI LS 100 luminescence spectrometer. For recording emission and excitation spectra, solutions were placed in quartz cuvettes while solids were ground finely and placed in 5 mm quartz tubes.

X-ray Structure Determinations. Yellow, roughly spherical crystals of $[Me_3P-Au-C\equiv C-C_6H_2Me_2-C\equiv C-Au-PMe_3]$ were grown from a mixture of CH_2Cl_2, $C_2H_4Cl_2$, MeCN, and *n*-pentane at room temperature. The diffraction experiments were carried out using a Siemens P4 diffractometer with XSCANS software package[17] using graphite-monochromated Mo Kα radiation at 23 °C. The cell constants were obtained by centering 24 high-angle reflections ($23.7 \le 2\theta \le 24.9°$). The Laue symmetry $2/m$ was determined by merging symmetry-equivalent reflections. A total of 3775 reflections were collected in the θ range 2.0−23.0° ($-1 \le h \le 21$, $-1 \le k \le 10$, $-13 \le l \le 13$) in ω scan mode at variable scan speeds (1−20 deg/min). Background measurements were made at the ends of the scan range. Four standard reflections were monitored at the end of every 297 reflection collected. An empirical absorption correction was applied to the data. The maximum and minimum transmission factors are 0.534 and 0.475, respectively. The space group $P2_1/c$ was determined from the systematic absences (h0*l*, $l = 2n + 1$ and 0k0, $k = 2n + 1$). The data processing, solution, and initial refinements were done using SHELXTL-PC[18] programs. The final refinements were performed using SHELXL-93[19] software programs. Anisotropic thermal parameters were refined for all the non-hydrogen atoms. The hydrogen atoms were included in the neutral molecule in the calculated positions and were included for the purpose of structure factor calculations only. In the final difference Fourier synthesis, the electron density ranged from 1.271 to −1.085 e Å^{-3}, of which the top four peaks were associated with Au atoms at distances of 1.03 and 1.27 Å. A secondary extinction coefficient was refined to 0.000 56(8). The experimental details and crystal data are in Table 1, selected bond distances and angles are in Table 2, and the positional and thermal parameters, bond distances and angles, the anisotropic thermal parameters, hydrogen atom coordinates, selected torsion angles, and selected weighted least-squares planes are given in the Supporting Information.

Orange-yellow, rod-like crystals of $[XyN\equiv C-Au-C\equiv C-C_6H_4-NO_2]$ were grown from a mixture of CH_2Cl_2 and *n*-pentane at room temperature. A long rod was cut along (0$\bar{1}$0) to the size 0.23 × 0.14 × 0.12 mm, mounted at the end of a glass fiber, and used for the experiments. The diffraction experiments were carried out as above. A total of 3625 reflections were collected in the θ range 2.0−25.0° ($-1 \le h \le 17$, $-1 \le k \le 8$, $-17 \le l \le 17$) in $\omega-2\theta$ scan mode at variable scan speeds (1−20 deg/min). At the end of the data collection, the faces of the data crystal were indexed, the distances between the faces were measured, and a Gaussian absorption correction was applied. The space group $P2_1/c$ was determined from the systematic absences (h0*l*, $l = 2n + 1$ and 0*k*0, $k = 2n + 1$). The data processing, solution, and refinement were carried out as above. In the final difference Fourier synthesis, the electron density fluctuates in the range from 0.574 to −0.810 e Å^{-3}, of which the top two peaks were associated with H(17A) at distances of 1.28 and 0.63 Å. The mean and the maximum shift/esd in the final cycles were 0.000 and −0.001, respectively. The experimental details and crystal data are in Table 1, selected bond distances and angles are in Table 3, while the positional and thermal parameters, bond distances and angles, the anisotropic thermal parameters, hydrogen atom coordinates, selected torsion angles, and selected weighted least-squares planes are given in the Supporting Information.

Table 1. Crystal Data and Experimental Details for 4 and 12

complex	**4**	**12**
formula, fw	$C_{18}H_{26}Au_2P_2$, 698.26	$C_{17}H_{13}N_2O_2Au_1$, 474.26
temperature	23 °C	23 °C
wavelength	0.710 73 Å	0.710 73 Å
cryst syst	monoclinic	monoclinic
space group	$P2_1/c$	$P2_1/c$
unit cell dimensions	$a = 19.996(2)$ Å	$a = 15.117(2)$ Å
	$b = 9.178(1)$ Å	$b = 7.0567(9)$ Å
	$c = 11.889(1)$ Å	$c = 14.935(2)$ Å
	$\beta = 93.62(1)°$	$\beta = 97.95(1)°$
volume	2177.6(4) Å^3	1578.0(4) Å^3
Z	4	4
density, calcd, obsd	2.130, 2.1(5) g·cm^{-3}	1.996, 2.02(5) g·cm^{-3}
absorption coeff	13.60 mm^{-1}	9.33 mm^{-1}
F(000)	1288	896
no. of independent reflns	3001	3625
goodness-of-fit on F^2[a]	1.022	1.033
final *R* indices[b] [$I > 2\sigma(I)$]	R1 = 0.0447	R1 = 0.0384
	wR2 = 0.1021	wR2 = 0.0760
R indices (all data)	R1 = 0.0621	R1 = 0.0722
	wR2 = 0.1106	wR2 = 0.0862

[a] GooF = $[\sum w(F_o2 - F_c2)^2/(n-p)]^{1/2}$, where *n* is the number of reflections and *p* is the number of parameters refined. [b] R1 = $\sum(||F_o| - |F_c||)/\sum|F_o|$; wR2 = $[\sum w(F_o^2 - F_c^2)^2/\sum wF_o^4]^{1/2}$.

Table 2. Selected Bond Distances (Å) and Angles (deg) for 4

Au(1)−Au(2)	3.1361(9)	Au(1)−P(1)	2.268(4)
Au(1)−C(1)	1.971(14)	C(1)−C(2)	1.21(2)
C(2)−C(3)	1.44(2)	C(3)−C(4)	1.39(2)
C(3)−C(6)	1.41(2)	C(4)−C(6)#1	1.39(2)
C(4)−C(5)	1.52(2)	C(6)−C(4)#1	1.39(2)
P(1)−C(8)	1.79(2)	P(1)−C(7)	1.80(2)
P(1)−C(9)	1.81(2)	Au(2)−P(2)	2.270(4)
Au(2)−C(10)	1.982(12)	C(10)−C(11)	1.21(2)
C(11)−C(12)	1.45(2)	C(12)−C(15)	1.39(2)
C(12)−C(13)	1.40(2)	C(13)−C(15)#2	1.39(2)
C(13)−C(14)	1.50(2)	C(15)−C(13)#2	1.39(2)
P(2)−C(16)	1.74(2)	P(2)−C(17)	1.77(2)
P(2)−C(18)	1.80(2)		
P(1)−Au(1)−Au(2)	92.7(1)	C(1)−Au(1)−P(1)	177.9(4)
C(1)−Au(1)−Au(2)	89.1(4)	C(2)−C(1)−Au(1)	177.1(12)
C(1)−C(2)−C(3)	176(2)	C(4)−C(3)−C(6)	118.2(12)
C(4)−C(3)−C(2)	120(2)	C(6)−C(3)−C(2)	121.3(14)
C(6)#1−C(4)−C(3)	118.8(14)	C(6)#1−C(4)−C(5)	120(2)
C(3)−C(4)−C(5)	121.5(14)	C(4)#1−C(6)−C(3)	123.0(13)
C(4)#1−C(6)−H(6)	118.5(10)	C(8)−P(1)−C(7)	102.9(8)
C(8)−P(1)−C(9)	103.4(12)	C(7)−P(1)−C(9)	106.1(10)
C(8)−P(1)−Au(1)	113.2(7)	C(7)−P(1)−Au(1)	115.6(5)
C(9)−P(1)−Au(1)	114.3(7)	P(2)−Au(2)−Au(1)	90.83(11)
C(10)−Au(2)−P(2)	175.6(4)	C(10)−Au(2)−Au(1)	93.4(4)
C(11)−C(10)−Au(2)	178.4(12)	C(10)−C(11)−C(12)	178.2(14)
C(15)−C(12)−C(13)	119.0(10)	C(15)−C(12)−C(11)	120.4(11)
C(13)−C(12)−C(11)	120.6(11)	C(15)#2−C(13)−C(12)	117.2(11)
C(15)#2−C(13)−C(14)	121.9(12)	C(12)−C(13)−C(14)	120.9(12)
C(16)−P(2)−C(17)	106.0(11)	C(16)−P(2)−C(18)	103.3(10)
C(17)−P(2)−C(18)	104.2(13)	C(16)−P(2)−Au(2)	113.1(6)
C(17)−P(2)−Au(2)	113.6(6)	C(18)−P(2)−Au(2)	115.6(7)

[a] Symmetry transformations used to generate equivalent atoms: #1, −x, −y, −z; #2, −x + 1, −y, −z.

Results and Discussion

The complexes **1**−**20**, which are all stable to air at room temperature,[14−16] have been studied. They can

(17) *XSCANS*; Siemens Analytical X-Ray Instruments, Inc.: Madison, WI,1990.
(18) Sheldrick, G. M. *SHELXTL-PC Software*; Siemens Analytical X-Ray Instruments, Inc.: Madison, WI, 1990.
(19) Sheldrick, G. M. *SHELXL-93*; University of Göttingen: Göttingen, Germany, 1993.

Table 3. Bond Distances (Å) and Angles (deg) for Complex 12

Au−(1)−C(9)	1.958(7)	Au(1)−C(1)	1.990(8)
C(1)−C(2)	1.188(10)	C(2)−C(3)	1.421(9)
C(3)−C(8)	1.383(12)	C(3)−C(4)	1.402(12)
C(4)−C(5)	1.368(12)	C(5)−C(6)	1.356(14)
C(6)−C(7)	1.368(13)	C(6)−N(2)	1.490(10)
C(7)−C(8)	1.387(11)	N(2)−O(1)	1.205(14)
N(2)−O(2)	1.224(13)	C(9)−N(1)	1.142(9)
N(1)−C(10)	1.402(8)	C(10)−C(11)	1.391(10)
C(10)−C(15)	1.409(10)	C(11)−C(12)	1.399(11)
C(11)−C(16)	1.514(11)	C(12)−C(13)	1.374(13)
C(13)−C(14)	1.345(13)	C(14)−C(15)	1.384(11)
C(15)−C(17)	1.493(11)		

C(9)−Au(1)−C(1)	177.8(3)	C(2)−C(1)−Au(1)	177.2(8)
C(1)−C(2)−C(3)	178.3(10)	C(8)−C(3)−C(4)	119.1(7)
C(8)−C(3)−C(2)	120.9(8)	C(4)−C(3)−C(2)	120.0(8)
C(5)−C(4)−C(3)	119.6(9)	C(6)−C(5)−C(4)	120.0(9)
C(5)−C(6)−C(7)	122.3(8)	C(5)−C(6)−N(2)	119.0(9)
C(7)−C(6)−N(2)	118.6(10)	C(6)−C(7)−C(8)	118.2(9)
C(3)−C(8)−C(7)	120.7(9)	O(1)−N(2)−O(2)	125.5(10)
O(1)−N(2)−C(6)	116.6(11)	O(2)−N(2)−C(6)	117.9(11)
N(1)−C(9)−Au(1)	174.3(7)	C(9)−N(1)−C(10)	172.3(8)
C(11)−C(10)−N(1)	119.8(7)	C(11)−C(10)−C(15)	123.9(7)
N(1)−C(10)−C(15)	116.3(7)	C(10)−C(11)−C(12)	116.2(7)
C(10)−C(11)−C(16)	120.4(7)	C(12)−C(11)−C(16)	123.4(8)
C(13)−C(12)−C(11)	121.0(8)	C(14)−C(13)−C(12)	120.7(8)
C(13)−C(14)−C(15)	122.7(9)	C(14)−C(15)−C(10)	115.5(7)
C(14)−C(15)−C(17)	124.0(8)	C(10)−C(15)−C(17)	120.5(7)

Chart 1

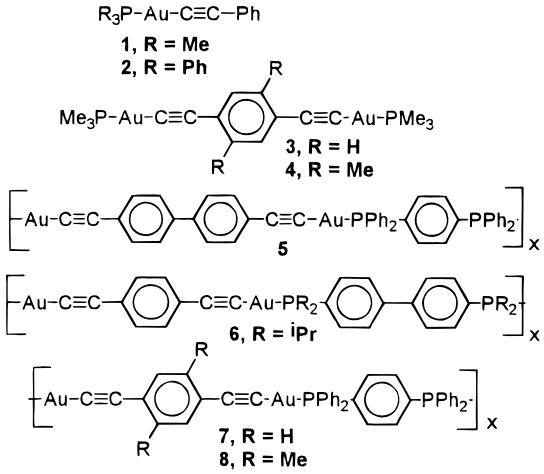

be classified broadly as phosphine−gold(I) acetylides (**1**−**8**, Chart 1) or isocyanide−gold(I) acetylides (**9**−**20**, Chart 2). Within each class, there are examples of mononuclear (**1**, **2**, **9**−**11**), binuclear (**3**, **4**, **13**−**15**), and oligonuclear or polynuclear complexes (**5**−**8**, **16**−**20**). The aim was to search for trends in the emission properties as a function of the stabilizing ligand (phosphine versus isocyanide), particularly as a function of the nuclearity of the complexes. It was also of interest to determine if trends in the solid state emission spectra could be correlated with the presence and strength of intermolecular Au···Au interactions (note that intramolecular interactions are of course not possible in these rigid-rod compounds). For this part of the study, it was desirable to have more structural information on the model complexes, and so the complexes **4** and **12** were characterized by X-ray structure determinations.

Molecular Structure of [Me_3P−Au−C≡C−C_6H_2-Me_2−C≡C−Au−PMe_3], 4. The unit cell of **4** contains two independent molecules, whose structures are shown in Figure 1; selected bond lengths and angles are presented in Table 2. Each molecule has a crystallographically-imposed center of symmetry. Bond parameters are discussed for only one of the independent molecules, but there are no significant differences for the other (Table 2). The C≡C bond length of 1.21(2) Å is similar to those found in other alkynylgold(I) compounds.[8,9,14−16] The Au−P bond distance of 2.268(4) Å is longer than those found in complexes of the type $ClAuPR_3$ (2.22−2.24 Å)[20] but similar to those found in

Chart 2

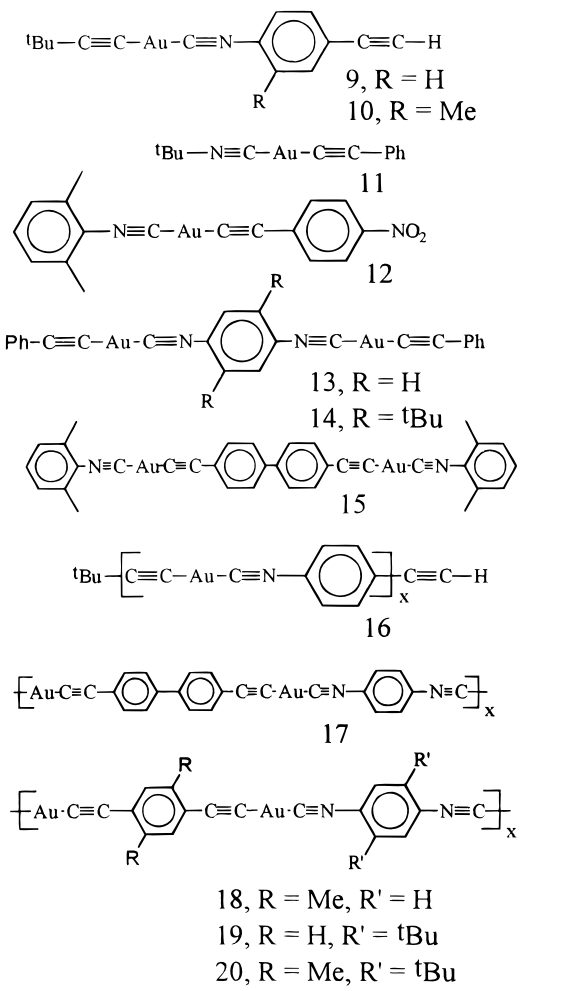

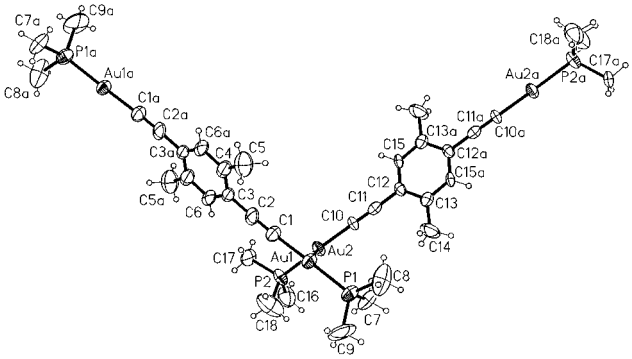

Figure 1. A view of the structures of the two independent molecules of the binuclear rigid rod complex **4**.

(20) (a) Balch, A. L.; Fung, E. Y.; Olmstead, M. M. *J. Am. Chem. Soc.* **1990**, *112*, 5181. (b) Eggleston, D. S.; McArdie, J. V.; Zuber, G. E. *J. Chem. Soc., Dalton Trans.* **1987**, 677. (c) Jones, P. G. *Acta Crystallogr.* **1980**, *36B*, 2775. (d) Bates, P. A.; Waters, J. M. *Inorg. Chim. Acta* **1985**, *98*, 125. (e) Cooper, M. K.; Henrick, K.; McPartlin, M.; Latten, J. *Inorg. Chim. Acta* **1982**, *65*, L185. (f) Schmidbaur, H.; Wohlleben, A.; Wager, F.; Orama, O.; Huttner, G. *Chem. Ber.* **1977**, *110*, 1748.

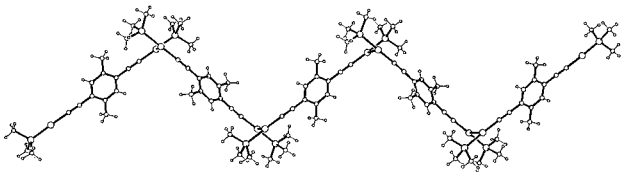

Figure 2. The intermolecular Au···Au contacts in **4**, leading to a polymeric zigzag chain structure.

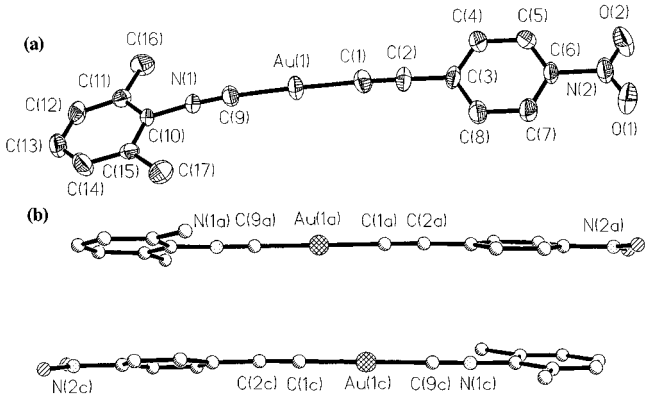

Figure 3. (a) A view of the structure of **12**. (b) A neighboring pair of molecules of **12**, showing the head-to-tail π-stacking.

other alkynyl derivatives.[8,9,15,20,21] For example, Au−P distances have been reported for Au(C≡CC$_6$F$_5$)PPh$_3$ = 2.274(1) Å,[20a] Au(C≡CCH$_2$OMe)P(C$_6$H$_4$−Me-4)$_3$ = 2.274(3) Å,[20b] and C$_2${AuP(C$_6$H$_4$Me-3)$_3$}$_2$ = 2.270(4), 2.284(3) Å,[20c] and these longer distances are indicative of the high *trans* influence of the alkynyl group. The Au−C bond distance of 1.97(1) Å is also unexceptional.[8,9,15,20] The angles C(1)−Au(1)−P(1), C(2)−C(1)−Au(1), and C(1)−C(2)−C(3) = 177.9(4)°, 177(1)°, and 176.0(2)°, respectively, deviate only slightly from linearity.

The most interesting feature of **4** is the packing of the molecules in the crystal lattice. The rod-like molecules are packed in zig-zag chains held loosely together through relatively short Au···Au interactions (Figure 2), thus, leading to a weakly bound polymeric structure in the crystal. The intermolecular Au···Au distance in **4** of 3.1361(9) Å is one of the shortest known in gold(I) acetylides.[8,9] However, there is no π-stacking of the aromatic rings in **4**, since the closest intermolecular distance between ring centroids is 9.18 Å. In this sense, the complex differs from the related complex [(Ph−C≡C−Au)$_2$(CN−C$_6$H$_2$(^{t}Bu)$_2$−NC)], **14**,[8] in which the closest distance is 4.35 Å between centroids of phenyl and C$_6$H$_2$tBu$_2$ groups and also from complex **12** discussed below.[14]

Molecular Structure of [XyNC−Au−C≡C−C$_6$H$_4$-NO$_2$], 12. The structure of **12** is shown in Figure 3; selected bond lengths and angles are presented in Table 3. As expected, the geometry about the gold(I) center is linear with a C9−Au1−C1 angle of 177.8(3)° and the angles C3−C2−C1, C2−C1−Au1, Au1−C9−N1, and C9−N1−C10 = 178(1)°, 177.2(8)°, 174.3(7)°, and 172.3(8)°, respectively, are also close to the ideal value of 180° for a rigid-rod molecule. The gold−carbon distances are

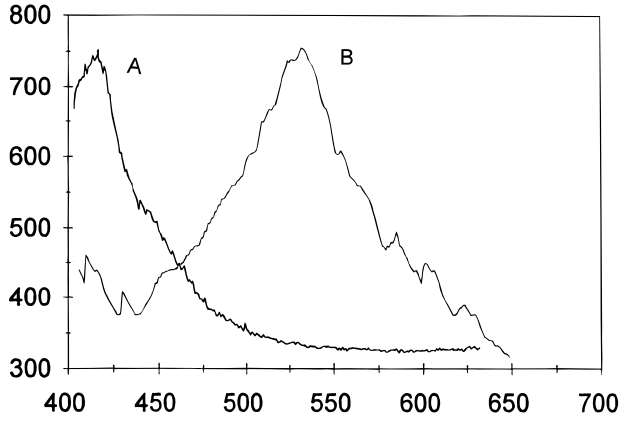

Figure 4. The emission spectra for complex **4** at 298 K; (A) in CH_2Cl_2 solution and (B) in the solid state.

similar to those in related gold(I) acetylides and isocyanide complexes.[8−10,14−16]

Figure 3 also illustrates the orientation of neighbouring molecules in the crystals of **12**. The closest intermolecular gold···gold contact is 3.92 Å, which is longer than the normal range of ca. 2.75−3.40 Å for such weak intermolecular bonds between Au(I) centers.[1] However, the distance between centroids of the aromatic rings of the 4-nitrophenylacetylide and xylyl isocyanide units in adjacent molecules of **12** is 3.722 Å with a dihedral angle of 0.9°. This suggests that there is π-stacking of the aryl groups, perhaps with the xylyl isocyanide as a π-donor and the 4-nitrophenylacetylide as a π-acceptor.

Luminescence Properties. The emission spectra of complexes **1**−**20** and some related compounds at $\lambda >$ 350 nm in the solid state (and dichloromethane solutions where solubilities allow) are summarized in Table 4. The phosphine and isocyanide derivatives will be discussed in turn.

The mononuclear complexes [Me$_3$P−Au−C≡C−Ph], **1**, and [Ph$_3$P−Au−C≡C-Ph], **2**, give intense emission at room temperature in the range 410−504 nm either in solution in dichloromethane or in the solid state when excited at 350 nm. The solid state spectra contain a single broad band, but the fluid phase spectra display a rich structure. The spectra are in good agreement with those reported independently.[8,9] The emission is proposed to occur from $^3(\pi-\pi^*)$ or $^3(\sigma-\pi^*)$ excited states associated with the Au−C≡CPh groups. In most other gold(I) compounds studied, the phosphine ligands contain aryl substituents and the π^* orbital involved is thought to be localized on the arylphosphine but, since compounds **1**, **3** and **4** contain trimethylphosphine ligands, the π^* orbital, in these cases at least, must be associated with the acetylide ligand.[8e,9c]

The binuclear complexes [Me$_3$P−Au−C≡C−C$_6$H$_4$−C≡C−Au−PMe$_3$], **3**, and [Me$_3$P−Au−C≡C−C$_6$H$_2$Me$_2$−C≡C−Au−PMe$_3$], **4**, also give strong emission at room temperature when excited at 350 nm. In solution, each emits at 415 nm and, by analogy with the spectra of **1** and **2**, this can be assigned to $^3(\pi-\pi^*)$ or $^3(\sigma-\pi^*)$ excited states associated with the digold diacetylide groups. However, in the solid state, the emission is observed at 540 nm, a dramatic red shift (Figure 4). Similar effects have been observed in other gold(I) complexes having short Au···Au contacts in the solid state, and the emission has usually been assigned to a $^3(d_\delta^*-p_\sigma)$ or $^3(d_\sigma^*-p_\sigma)$ excited state.[8a−f,9c] This is consistent with the

(21) (a) Alejos, P.; Coco, S.; Espinet, P. *New J. Chem.* **1995**, *19*, 799. (b) Whittall, I. R.; Humphrey, M. G.; Houbrechts, S.; Persoons, A.; Hockless, D. C. R. *Organometallics* **1996**, *15*, 5738. (c) Whittall, I. R.; Humphrey, M. G.; Samoc, M.; Luther-Davies, B. *Angew. Chem., Int. Ed. Engl.* **1997**, *36*, 370.

Table 4. Photophysical Data and Au···Au Distances for the Complexes[a]

compound	medium	λ_{ex}/nm	λ_{em}/nm	d(Au···Au)/Å
1	solid	350	455	
	CH_2Cl_2	350	424,450,504	
2	solid	350	459	3.379
	CH_2Cl_2	350	410,454	
3	solid	350	540	
	CH_2Cl_2	350	415	
4	solid	350	540	3.136
	CH_2Cl_2	350	415	
5	solid	380	600	
6	solid	380	600	
7	solid	380	600	
8	solid	380	600	
9	solid	380	461	
	CH_2Cl_2	350	429	
10	solid	380	460	3.479
	CH_2Cl_2	350	432	
11	solid	350	470	
12	solid	430	633	3.923
	CH_2Cl_2	380	503	
13	solid	380	550	
14	solid	383	501	3.176
15	solid	433	550	
16	solid	350	585	
17	solid	350	585	
18	solid	350	585	
19	solid	350	585	
20	solid	350	585	

[a] All spectra were recorded at 298 K.

observation of a short Au···Au contact of 3.163(1) Å in **4**, which is not present in solution, but the assignment will be discussed further below. The emission spectra of the related complex [(4-MeC_6H_4)$_3$P−Au−C≡CC_6H_4-C≡C−Au−P(4-MeC_6H_4)$_3$], with a tritolylphosphine ligand in place of trimethylphosphine, has been reported recently.[9c] The solution phase emission is red shifted compared to **3**, perhaps indicating involvement of the π*-orbitals of the arylphosphine groups in the excited state,[9c] but the solid phase emission is blue shifted, presumably indicating weaker Au···Au interactions with the bulkier phosphine substituents.

Since the polymers **5**−**8**, with gold(I) centers bridged by both diacetylides and diphosphines, are insoluble; they could only be examined in the solid state. The solid state emission spectra of **5**−**8** all exhibit a weak, broad structureless band centered near 600 nm when excited at 350 or 380 nm. There is a sequential red shift in the solid state emission spectra from the mononuclear to the binuclear and polynuclear complexes. The emission at 600 nm for the polymers can be taken to indicate the presence of intermolecular Au···Au interactions in the solid state,[8,9] and the red shift compared to **1**−**4** indicates that the excited state is stabilized by the greater degree of delocalization in the conjugated polymers. The red shift and reduced intensity observed in the emission bands of **5**−**8** compared to **3** and **4** are attributed to the greater delocalization in the polynuclear compared to the dinuclear complexes. However, we cannot rule out the possibility that the shifts are related to the number and/or strength of the Au···Au interactions in the polymers.

Similar trends to those discussed above were observed for the isocyanide complexes **9**−**20** (Table 4 and Figure 5), though, in general, the emissions were less intense than for the corresponding phosphine complexes. The mononuclear complexes **9**−**11** display emissions between ca. 420−470 nm, with a relatively small red shift

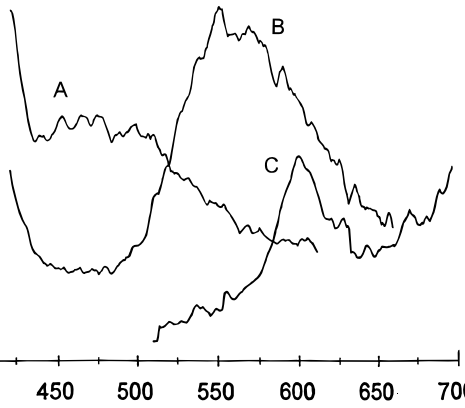

Figure 5. Emission spectra of complexes (A) **11**, (B) **15**, and (C) **20** in the solid state at 298 K, showing the red shift as the molecular size increases.

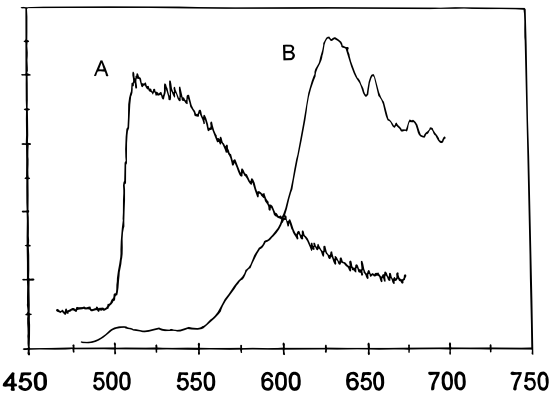

Figure 6. The emission spectra of complex **12** at 298 K; (A) in CH_2Cl_2 solution and (B) in the solid state.

between solution and solid state spectra, and these bands are again assigned to $^3(\pi-\pi^*)$ or $^3(\sigma-\pi^*)$ excited states. It is not clear if the π, π* states are mostly associated with the isocyanide or the acetylide groups, especially when both contain aryl substituents. The binuclear complexes **13**, **14**, and **15**, having bridging diisocyanide and diacetylide ligands give solid state emission at 501, 550, and 550 nm, respectively, but are very weakly emissive at room temperature in dichloromethane solution. The emission energies are consistent with the presence of Au···Au interactions in the solid state, and this has been proved for **14** (Au···Au = 3.176 Å) by an X-ray structure determination.[14] The insoluble oligomers or polymers **16**−**20** all give weak, broad emissions at 585 nm. Again, this indicates that intermolecular Au···Au interactions are present in the solid state structures, and the red shift compared to **13**−**15** is attributed to the greater degree of electron delocalization in the extended rigid-rod molecules.

The most intense emission observed in the isocyanide complexes was for the mononuclear complex [XyN≡C−Au−C≡C$C_6H_4NO_2$], **12**. For a solution in CH_2Cl_2, an intense emission was observed at 503 nm, and this was red shifted to 633 nm in the solid state (Figure 6). The large red shift is surprising since the closest intermolecular Au···Au contact is 3.92 Å in the crystalline state, too long for a bonding interaction. Qualitatively, the large shift must be attributed to the π-stacking of the aromatic rings of the xylyl and 4-nitrophenyl groups in the crystal. The lower energy of the solution phase emission compared to **9**−**11** is attributed to the presence of the 4-nitro substituent in **12**, which is electronegative

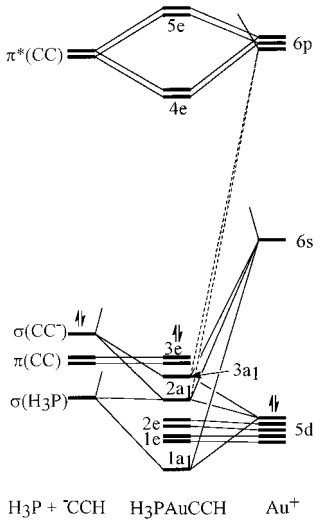

Figure 7. An energy correlation diagram for formation of $H_3PAuCCH$ from the fragments H_3P, $HC{\equiv}C^-$, and Au^+.

and gives a more delocalized π-system and, hence, a significantly lower energy of the first π^* orbital. It is particularly striking that the two complexes, which have been structurally characterized in this work, both show a large red shift in the emission spectra on going from solution to the solid state (Figures 4 and 6), but **4** has intermolecular Au···Au interactions but no π-stacking, whereas **12** has intermolecular π-stacking but probably no significant Au···Au interactions.

Discussion

There are a number of interesting conclusions that can be drawn from the above observations. First, the trend of a red shift on going from mononuclear to binuclear to polynuclear gold(I) acetylides (Figure 5) does support the view that there is at least some conjugation in the molecules. That feature was part of the molecular design but, since conjugation relies on $d_\pi-p_\pi$ and with the diphosphine derivatives on $d_\pi-d_\pi$ overlap as well as $p_\pi-p_\pi$ overlap, it was not obvious that real conjugation could be achieved. This might be important if derivatives are to be used in liquid crystal devices, for nonlinear optics, or other optical applications.[21] Second, the empirical trends indicate that there are close intermolecular contacts in the polymeric compounds between gold(I)..gold(I) centers and/or between π-bonded arylethynyl/aryl isocyanide groups. Most previous work has suggested that the large red shift on going from solution to solid phase emission is indicative of short gold(I)..gold(I) contacts, but complex **12** provides an example where there is a large red shift for a molecule with a long Au···Au separation but shorter π-stacking interaction. In order to gain some insight into this issue as well as to try to understand why the emissions in solution are dominated by $\pi-\pi^*$ or $\sigma-\pi^*$ excited states while in the solid phase d−p excited states are dominant, some EHMO (extended Hückel molecular orbital) calculations were carried out.

The calculations have been carried out for model compounds $H_3P-Au-C{\equiv}CH$, $H_3P-Au-C{\equiv}C-Ph$, $HN{\equiv}C-Au-C{\equiv}CH$, and $PhN{\equiv}C-Au-C{\equiv}CPh$, but the principles can be understood in terms of the first molecule only. Figure 7 shows an energy correlation diagram for formation of $H_3P-Au-C{\equiv}CH$ from Au^+ with PH_3 and $HC{\equiv}C^-$. The calculation indicates that the HOMO (highest occupied molecular orbital) is the degenerate $\pi(C{\equiv}C)$ orbitals 3e, with an orbital $3a_1$ having mostly $\sigma(Au-C)$ character very close in energy. There are five orbitals $2a_1$, 2e, and 1e having mostly gold d-character and then the mostly $\sigma(Au-P)$ orbital $1a_1$. As has been discussed elsewhere, the $\sigma(Au-L)$ orbitals are not derived from simple sp hybridized orbitals on gold but contain much gold $5d_{z^2}$ character also, as is clearly indicated in Figure 7.[22] There is also mixing of the relative orbital contributions to the three occupied a_1 orbitals, and so the descriptions as σ(AuP), σ(AuC), and d_{z^2} are only rough approximations to the true picture (Figure 7). The LUMO (lowest unoccupied molecular orbital) is a degenerate orbital 4e having both Au $6p_\pi$ and $\pi^*(C{\equiv}C)$ character, as shown in **A**, Chart 3. Thus, the lowest energy excited state is expected to arise from excitation of an electron from either the π-$(C{\equiv}C)$ or $\sigma(Au-C)$ orbital to the 4e orbitals, which may be described as mixed π^*(CC) and Au 6p character. Of course, this is consistent with the assignments given above for the unassociated molecules, with the complication of mixing of the π^*(CC) and Au 6p character.

Chart 3

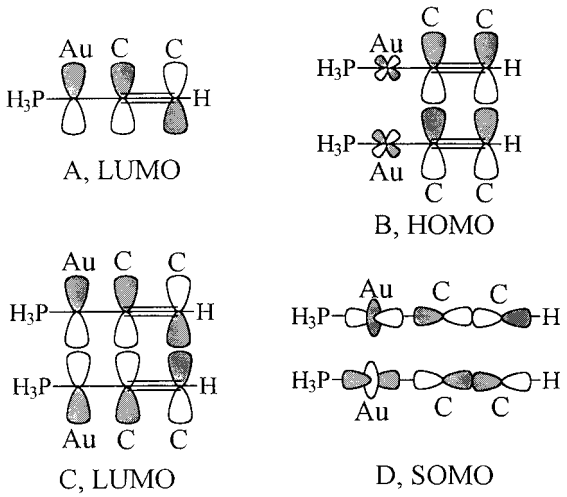

To mimic the solid state structures, calculations were carried out with two $H_3P-Au-C{\equiv}CH$ molecules with their molecular axes parallel, with gold(I) centers separated by 3 Å and with the dihedral angle between AuCCH vectors ranging from 0−180°. Naturally, pairs of MOs of the same symmetry on adjacent molecules interact, the result being that the HOMO is at higher energy and the LUMO at lower energy. For the case where the dihedral angle between AuCCH vectors is zero, the HOMO and LUMO are shown as **B** and **C**; the HOMO is the antibonding combination of filled $\pi(CC)_x$ MOs, and the LUMO is the bonding combination of the mixed $\pi^*(CC)_x + 6p_x(Au)$ orbitals. The SOMO is the antibonding combination of σ(AuC) levels, and this takes on a stronger antibonding component derived from the gold $5d_{z^2}$ component, as illustrated in **D** (counterbalanced still by the bonding components from Au 6s and $6p_z$ orbitals). As the dihedral angle between AuCCH vectors increases, the intermolecular π(CC) and π^*(CC) interactions decrease rapidly but the gold(I) orbitals still interact strongly. The energy correlation diagram for

(22) Bancroft, G. M.; Chan, T.; Puddephatt, R. J.; Tse, J. S. *Inorg. Chem.* **1982**, *21*, 2946.

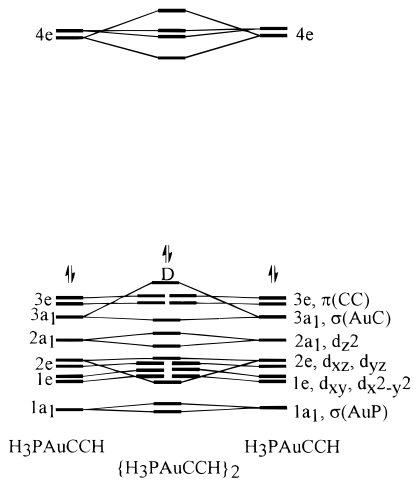

Figure 8. An energy correlation diagram for formation of $(H_3PAuCCH)_2$ from two molecules of $H_3PAuCCH$, with the dihedral angle CAuAuC = 90°. The HOMO is now the antibonding combination of σ(AuC) levels with a strong σ*-(Au d_{z^2}−C $2p_z$) component illustrated as D.

interaction of two $H_3P-Au-C\equiv CH$ molecules with the dihedral angle at 90° is shown in Figure 8. In the absence of interactions between π(CC) and π*(CC) orbitals, the HOMO is now calculated to be the antibonding combination of the two σ(AuC) orbitals; indeed, there is some rehybridization which gives the HOMO more character of the σ*(d_{z^2}) orbital and the LUMO a higher degree of Au 6p character than in the monomer. The assignment of the emission as arising from a d_σ*−p_σ excited state (here σ refers to the Au···Au vector) under these conditions is therefore not unreasonable, although it is perhaps only part of the picture. It should be clear from this discussion that a red shift in the solid state is expected either if there is a short Au···Au contact or if there is a strong π-stacking effect between unsaturated groups, though the assignment may be different. It is not always obvious why intermolecular Au···Au contacts are sometimes observed and sometimes not. In the case of complex **12**, it is likely that there is a competition between maximizing Au···Au bonding or π-stacking and that, in the special case of the 4-nitrophenyl substituent, the π-stacking is dominant.

Acknowledgment. We thank the N.S.E.R.C. (Canada) for financial support and Dr. S. W.-K. Choi for valuable advice.

Supporting Information Available: Tables of crystal data and experimental details, positional and thermal parameters, bond distances and angles, anisotropic thermal parameters, and hydrogen atom coordinates for complexes **4** and **12** (10 pages). Ordering information is given on any current masthead page.

OM970256M